





Review of Differential Power Processing Converter Techniques for Photovoltaic Applications

Hoejeong Jeong , Student Member, IEEE, Hyunji Lee , Student Member, IEEE, Yu-Chen Liu , Senior Member, IEEE, and Katherine A. Kim , Senior Member, IEEE

Abstract—Differential power processing (DPP) converters are utilized in photovoltaic (PV) power systems to achieve high-efficiency power output, even under uneven lighting or mismatched PV cell situations. Since this DPP concept has been introduced for PV systems, various topologies and control algorithms have been proposed and validated, showing the benefits of DPP converters systems over existing series string and full power processing converter solutions. However, DPP systems are highly coupled and can be challenging to control. Various architectures, topologies, and control strategies for both series and parallel DPP architectures are reviewed and compared. Tradeoffs of different DPP converters and topologies are discussed. Also, the power curve for the PV connected to bus, PV to PV, and PV to independent port series DPP architectures are evaluated in terms of inverter interaction. To date, the PV to PV series DPP systems have been most widely implemented and robust system-level control for all architectures has been a major research focus. Furthermore, research and development is still needed, particularly for commercialization and parallel DPP approaches for emerging PV applications.

Index Terms—Photovoltaic systems, differential power processing (DPP), partial power processing, dc-dc converter, sub-module converter, system control.

I. INTRODUCTION

THE installation of photovoltaic (PV) power systems has been increasing steadily over recent years on a global scale [1]. Utility-scale and residential grid-connected PV systems are widely used to provide renewable energy to the grid, but there are also emerging PV applications, such as solar-powered internet of things and wearable devices [2]. In most applications, PV cells or panels are connected in series to achieve the higher voltages required by the application, as shown in Fig. 1a. However, series strings of PV cells often experience severe power decrease when there is mismatch in the PV cells' electrical characteristics, often

Manuscript received April 11, 2018; revised August 26, 2018; accepted October 9, 2018. Date of publication October 30, 2018; date of current version February 26, 2019. This work was supported in part by the Basic Science Research Program through the National Research Foundation of Korea (NRF) funded by the Ministry of Education under Grant 2016R1D1A1B03931573 and in part by the Research funding from the Ulsan National Institute of Science and Technology under Grant 1.180038.01. Paper no. TEC-00440-2018. (Corresponding author: Katherine A. Kim.)

H. Jeong, H. Lee, and K. A. Kim are with the School of Electrical and Computer Engineering, Ulsan National Institute of Science and Technology, Ulsan 44919, South Korea (e-mail: hjeong94@unist.ac.kr; LEEHJ1004@unist.ac.kr; kkim@unist.ac.kr).

Y.-C. Liu is with the Department of Electrical Engineering, National Ilan University, Yilan 260, Taiwan (e-mail: ycliu@niu.edu.tw).

Color versions of one or more of the figures in this paper are available online at <http://ieeexplore.ieee.org>.

Digital Object Identifier 10.1109/TEC.2018.2876176

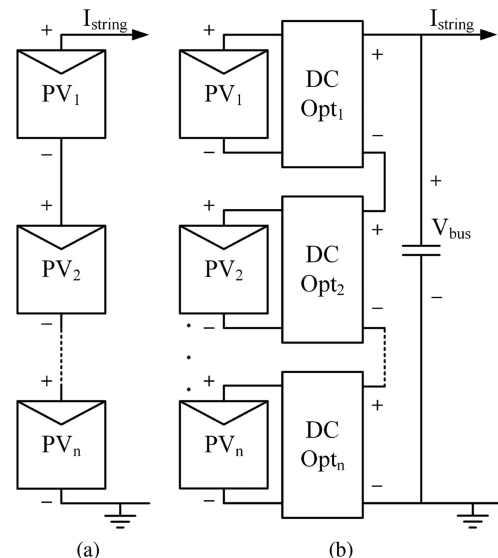


Fig. 1. PV systems using (a) series string and (b) dc optimizers.

caused by partial shading, panels at different tilt angles, dust accumulation, or cell degradation [3]–[5].

To overcome this severe power reduction due to series connection, the concept of individual converters was introduced which connected each PV panel to an individual converter controlling the PV panel's operation. Examples of this kind of system architecture are cascaded converters [6], dc optimizers [7], and microinverters [8]. With this type of system architecture, each converter is typically able to achieve maximum power point tracking (MPPT) on each PV panel. However, individual MPPT for each PV is not possible in some conditions, due to the limited voltage conversion ratio of the dc-dc converter topology and the finite voltage or current ratings of the power stage devices [9]. For effective system-level control, it is necessary to adopt both distributed MPPT and central MPPT [10]. An illustration of dc optimizers used in a PV system is shown in Fig. 1b. In these architectures, the converter processes all the PV power, which is referred to as full power processing (FPP) [11]. Because the full PV power is processed through the converter, losses are proportional to the produced PV power. While FPP converters are effective against mismatch, more recently, an improved method that has lower power losses has been introduced.

The term *differential power processing* (DPP) for PV systems was introduced in [12] and patented in [13]. However, the basic PV DPP concept was introduced earlier in [14], which

applied battery cell balancing techniques to achieve DPP and offset losses from partial shading of a PV string. DPP converters are used to control *PV elements*, which are either PV panels, sub-panel strings, or individual PV cells. DPP converters process only the difference in power between a PV element and adjacent elements, while maintaining individual control of the PV elements. Here, the term *architecture* refers to the electrical connections between the PV elements and DPP converters, and *topology* refers to the circuit topology of the DPP converter, e.g., buck, boost, flyback.

DPP systems for PV systems can be divided into two categories of DPP architectures: series and parallel. Series DPP architectures maintain the series connection between PV elements, and DPP converters provide the required current difference between adjacent PV elements. These architectures are appropriate for applications that require an output voltage multiple times higher than that of the PV element, such as grid-tied PV inverter systems. The major sub-categories of series DPP architectures are PV connected to bus (PV-bus), PV connected to PV (PV-PV), and PV connected to an isolated port (PV-IP). Conversely, in parallel DPP architectures, the DPP converters provide the required voltage difference between the PV element and a common bus. The parallel DPP architecture is more appropriate for applications that require a voltage close to that of the PV element.

Since the concept's introduction, numerous DPP PV systems have been implemented and verified to show significant output power improvement compared to the series string connection and FPP systems, in both even lighting and partial shading conditions. Further, since only partial power is processed, the converter power rating can be a fraction of the PV panel's rating, which reduces converter cost, passive component size, and required board area [11], [12]. Further, studies in [15] have shown that replacing bypass diodes with DPP converters increased reliability by reducing the probability of reverse-bias and hot spotting problems in PV cells. FPP architectures exhibited a reduction rate in hot spotting events of 100%, while DPP architectures exhibited a comparable reduction rate of 93% [15].

To achieve the performance benefits of DPP converters in PV systems, recent research has focused on developing various architectures and topologies, improving converter design, and designing effective and reliable system control strategies. However, each DPP architecture has limitations and trade-offs. This paper is organized as follows: Section II details four main subcategories of series DPP architectures and their operation, as well as analyzes the interaction with a string-level inverter; Section III details the parallel DPP architecture and its operation; and Section IV concludes the paper.

II. SERIES DPP ARCHITECTURES

A. PV to Bus

In the series DPP PV-bus architecture, each DPP converter is connected between a PV element and the system bus, as shown in Fig. 2. Each PV element has a bidirectional DPP converter that can supply or remove current needed to maintain MPP operation of the PV element. For an ideal system of n PV elements, the

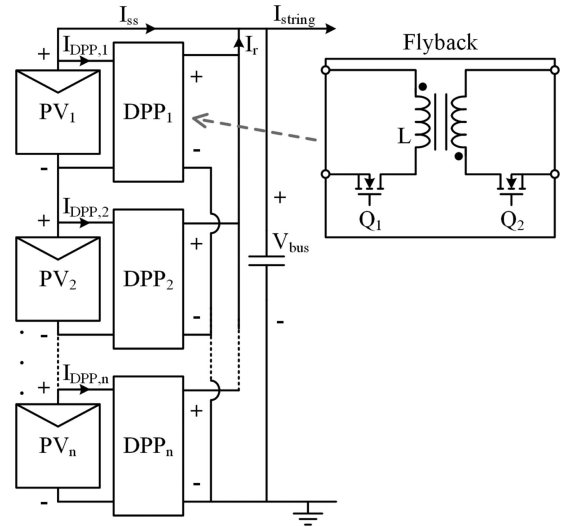


Fig. 2. Series DPP PV-bus architecture with flyback DPP converters.

PV current is determined by

$$I_{ss} = I_{PV,k} - I_{DPP,k} \quad (1)$$

for $k = 1, 2, \dots, n$, where I_{ss} is substring current, $I_{PV,k}$ is the k th PV current, and $I_{DPP,k}$ is the input current for the k th PV current. The return current I_r is determined according to

$$I_r = \sum_{k=1}^n \frac{V_{PV,k} I_{DPP,k}}{V_{bus}} \quad (2)$$

where $V_{PV,k}$ is the k th PV voltage and V_{bus} is the string bus voltage. Then, the string current I_{string} is

$$I_{string} = I_{ss} + I_r \quad (3)$$

The PV-bus DPP system is highly coupled and return current I_r is directly linked to the inverter string current I_{string} , which makes the interaction with the string-level inverter a challenge. This is further detailed in Section II-D.

For proper operation, the PV-bus DPP converter topology must not be a direct topology, where the negative of input and output are directly connected; typically, an isolated topology is chosen for the DPP converter. The MPPT of each PV is achievable at multiple string current values, but there is a unique minimum where the least amount of power is processed; this is the target operating point for the system [12]. Operating at this point reduces power losses and achieves higher output power than FPP converters [21].

Although this architecture was introduced in early DPP literature, the original PV-bus concept has not been widely implemented in the literature. Some works have suggested the boost topology for the DPP converter [12], [22]. However, upon closer inspection, it is not a true DPP topology. The main switch of the boost topology is connected to ground such that the converter sees the full voltage of its associated PV element and all elements below it. Although the topology allows for MPPT of each PV element, it is not an effective topology for DPP converters.

For the PV-bus architecture, if a flyback topology is used for the DPP converter, the turns ratio of the coupled inductor

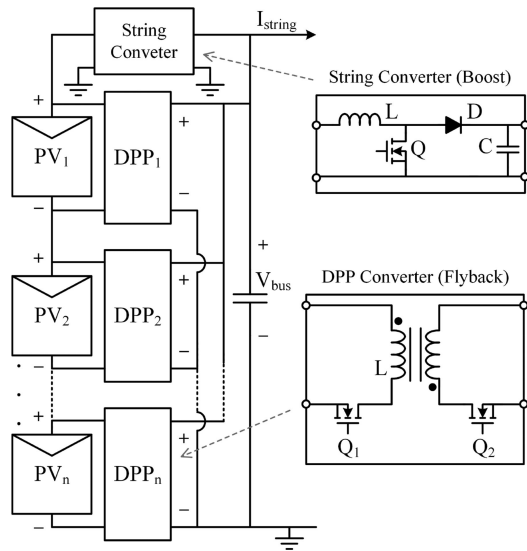


Fig. 3. PV-bus-direct architecture with flyback DPP converters.

can be used to scale the input-output voltage ratio based on the PV and bus voltages. Work in [16] utilizes a flyback as the DPP converter, but only as a unidirectional converter delivering power from the bus to the PV elements. The control strategy allows for exact MPPT of each PV element implemented for real-time distributed coordination and low computational overhead, but bidirectional power flow is needed to minimize power processed through the converters and optimize output power. A bidirectional flyback topology has also been proposed [12] but it has not been implemented and experimentally tested for the PV-bus architecture in the literature. A comprehensive simulation study of power-limited PV-bus converters in [21] identified power ratings of 15–17% of the PV element power to be effective against mismatch caused PV cell degradation.

There are also variations of the PV-bus architecture, such as [17] and [18], which is actually a unidirectional bus-to-PV DPP architecture. The converter topologies have been shown using a stacked LLC resonant converter driven by two switches [17] and a multi-stacked SEPIC converter with only one switch [18]. The multiple stacked converters are driven by just one or two switches, which reduces the amount of active parts and simplifies the control. However, the topologies only allow for voltage equalization of the PV elements, rather than exact MPPT. Also, due to the unidirectional nature of the converters, more power is processed than with bidirectional DPP converters, but it is still effective compared to series PV strings or FPP converters.

Another variation of the PV-bus architecture is the PV-bus-direct architecture, shown in Fig. 3, which utilizes a string dc-dc (boost) converter to control the PV substring current and connects the output of the DPP converters directly to the string converter output voltage bus [19]. This allows the string current to be directly controlled by the string dc-dc converter. The main string power is processed through this converter, which increases converter losses compared to the original PV-bus architecture, but the advantage is the decoupling of the substring current on the input side and the inverter string current on the output side. Because string converter can independently control the

substring current, the system more reliability maintains optimal power operation without being directly affected by changes in the inverter string current.

A bidirectional flyback topology with individual MPPT PV control for the DPP converters has been shown in [19], [20]. At the system control level, the string boost converter can implement a least power point tracking (LPPT) algorithm, which operates at the string current that minimizes power processed through all DPP converters [19], or a unit LPPT, which operates at the string current that minimizes the worst-case power processed through any one DPP converter [20].

The PV-bus implementation details are summarized in Table I. In order to simplify control, most of the implementations have either implemented unidirectional DPP converters or used the PV-bus-direct architecture. One challenge in designing PV-bus DPP converters is the high voltage step-up ratio from the PV- to bus-side. In a string of n PV elements, the output voltage of the DPP converters should be rated at n times the input voltage. While this is reasonable for small numbers, it becomes problematic for long strings of PV elements. Another challenge is the lack of scalability. Once a converter is designed and optimized for a set voltage ratio, the system cannot significantly increase the number of PV elements without redesigning the DPP converter.

B. PV to PV

In the series DPP PV-PV architecture, each DPP converter is connected between one PV element and another PV element, as shown in Fig. 4. Each DPP converter is bidirectional and can supply or remove current needed to maintain MPP operation of one of the PV elements. For a string of n PV elements, there are $n - 1$ DPP converters, where each DPP converter controls one PV at its MPPT. However, one of the PV elements is not controlled by a DPP converter, but by the the PV string current of the system. Let the duty ratio of the k th DPP converter be

$$D_k = \frac{V_{PV,k}}{V_{PV,k-1} + V_{PV,k}} \quad (4)$$

Then, operation of an ideal PV-PV system is best expressed in matrix form as in (5) shown at the bottom of next page, where $I_{DPP,k}$ is as labeled in Fig. 4. This system is also highly coupled, as shown in (5) shown at the bottom of next page, such that effective controllers must be carefully designed. The PV string current I_{string} that maximizes the power produced by all PV elements, including the one without a dedicated DPP converter, is the target operating point of the system. For given conditions of the PV elements, there is one unique PV string value that will achieve optimal power generation [12].

For the PV-PV DPP converter topology, a bidirectional switched-inductor is most commonly used [12], [14], [22], [26], [27], which can also be thought of as a bidirectional buck-boost converter and is referred to as a delta converter in [24], [25]. An alternate topology for the DPP converter is a resonant switched-capacitor converter [28]–[30], which allows for zero voltage switching and higher efficiency over a wider operating range. Work in [23] proposes a type of unidirectional DPP converter

TABLE I
COMPARISON OF SERIES DPP PV-BUS ARCHITECTURES

Type	Power Flow	Topology	Control	References
From bus to PV	unidir.	flyback	exact MPPT	[16]
From bus to PV	unidir.	multi-stacked LLC resonant	V balancing	[17]
From bus to PV	unidir.	multi-stacked SEPIC	V balancing	[18]
PV-bus-direct	bidir.	flyback	exact MPPT/LPPT	[19]
PV-bus-direct	bidir.	flyback	exact MPPT/Unit-LPPT	[20]

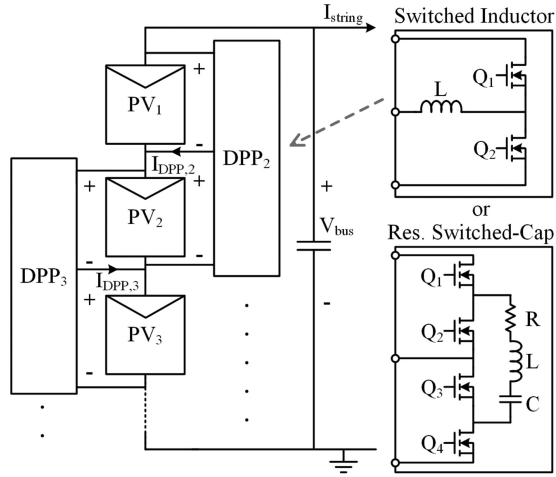


Fig. 4. Series DPP PV-PV architecture with switched inductor or resonant switched-capacitor DPP converters.

for voltage balance of sub-panel PV elements that uses a single inductor to reduce magnetic components. All PV-PV topologies are non-isolated topologies that can be implemented in small packages and at relatively low cost, both of which are primary concerns in the PV industry.

The main advantage of the PV-PV DPP converter is that the converter is rated based on the voltage characteristics of the PV element, such that it is independent of the main bus voltage. However, work in [21] showed that the maximum power processed in any DPP converter increases with PV string length, such that the required current rating of the DPP converter increases with PV string length. Still, PV-PV DPP converters have more potential for scalability than the PV-bus architecture. For PV-PV converters, the MPPT control algorithm should also be distributed to allow for easy scalability, however this is a non-trivial problem. Thus, much research on PV-PV converters has focused on distributed control algorithms.

In terms of control, work in [23], [28]–[30] focuses on voltage balance using low-complexity control techniques to achieve control near the MPP of the PV element while the string interacts with an inverter running standard MPPT algorithms. Work in [12] tested both constant voltage control and perturb and observe (P&O) MPPT control in the DPP converter coupled with a slower P&O MPPT at the string level [31]. The voltage reference control in the DPP converter requires fewer sensors and simpler control but only achieves near MPPT, while P&O achieves exact MPPT but requires more sensors and a digital controller. Work in [30] applied PV-PV converters to a dc microgrid application, where voltage balancing mode was utilized to achieve near-MPP operation during islanding mode and P&O MPPT for exact-MPP operation during grid-connected mode. Also, studies of power-limited PV-PV converters in [21] identified power ratings at 23–33% of the PV element power to be effective against power loss from long-term degradation.

Recent research has also focused on convergence to maintain maximum power point (MPP) operation for all PV elements. Work in [29] implemented a hill climbing MPPT for each resonant switched capacitor DPP converter, achieving exact MPPT. The algorithm was verified with 10 PV panels and 9 DPP converters, but convergence was on the minute time scale. Work in [26] focused on developing an algorithm for distributed control where the string-level converter used a slow-changing current-based P&O control while the DPP converters implemented a faster control loop. The DPP converter algorithm involved two perturbations and information exchange between neighboring converters, and was verified to be an effective distributed control for larger-scale systems. Alternatively, work in [27] implements a double-stage time-sharing MPPT approach where the algorithms for all converters are implemented on one digital controller. Both the DPP and string-level converters use a voltage-based P&O algorithm, but the control strategy coordinates their tracking. Experimental results show that it is effective against sudden irradiance changes, but its ability to scale up is

$$\begin{bmatrix} 1 & D_{n-1} - 1 & 0 & \dots & 0 \\ -D_n & 1 & D_{n-2} - 1 & \ddots & \vdots \\ 0 & -D_{n-1} & \ddots & \ddots & 0 \\ \vdots & \ddots & \ddots & 1 & 0 \\ 0 & \dots & 0 & -D_2 & 1 \end{bmatrix} \begin{bmatrix} I_{DPP,n} \\ I_{DPP,n-1} \\ \vdots \\ I_{DPP,2} \\ -I_{string} \end{bmatrix} = \begin{bmatrix} I_{PV,n-1} - I_{PV,n} \\ I_{PV,n-2} - I_{PV,n-1} \\ \vdots \\ I_{PV,1} - I_{PV,2} \\ -I_{PV,1} \end{bmatrix} \quad (5)$$

TABLE II
 COMPARISON OF SERIES DPP PV-PV ARCHITECTURES

Flow	Topology	PV Control (MPPT accuracy)	String Control	Exp. Setup	Ref.
unidir.	single swit. ind.	V balance (near)	hill climb	4 PV, 4 DPP Conv.	[23]
bidir.	swit. ind.	V reference (near) or P&O (exact)	P&O	3 PV, 2 DPP Conv.	[12]
bidir.	swit. ind.	V balance (near)	Panel: V balance	18 PV, 18 DPP Conv.	[24]
bidir.	swit. ind.	V balance (near)	unspecified MPPT	2 PV, 1 DPP Conv.	[25]
bidir.	swit. ind.	distrib. fast-loop current P&O (exact)	slow-loop current P&O	6 PV, 5 DPP Conv.	[26]
bidir.	swit. ind.	centralized voltage P&O (exact)	centralized voltage P&O	3 PV, 2 DPP Conv.	[27]
bidir.	res. swit. cap.	V balance (near)	unspecified MPPT	12 PV, 11 DPP Conv.	[28]
bidir.	res. swit. cap.	hill climb (exact)	manual	10 PV, 9 DPP Conv.	[29]
bidir.	res. swit. cap.	grid-connected: P&O (exact) islanded: V balance (near)	grid-connected: P&O islanded: none	3 PV, 2 DPP Conv.	[30]

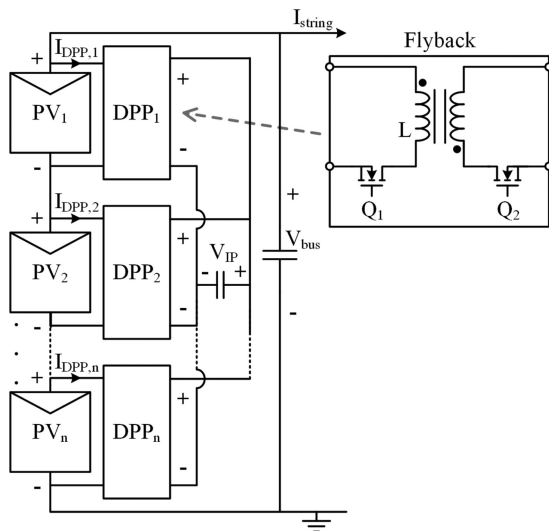


Fig. 5. Series DPP PV-IP architecture with flyback DPP converters.

limited. The PV-PV converter and control implementation details are summarized in Table II, where the experimental setup column details the number of PV elements and number of DPP converters used in experimental validation.

C. PV to Isolated Port

In the series DPP PV-IP architecture, also called PV-to-virtual-bus [12], each DPP converter is connected between a PV element and an independent isolated bus, as shown in Fig. 5. Each PV element has a bidirectional DPP converter that can deliver power to or from the isolated port to optimize PV power. The power into and out of the isolated port must be balanced such that an ideal system must follow

$$\sum_{k=1}^n V_{PV,k} I_{DPP,k} = 0 \quad (6)$$

where $I_{DPP,k}$ is as labeled in Fig. 5. Then, the string current is defined as

$$I_{string} = I_{PV,k} - I_{DPP,k} \quad (7)$$

for $k = 1, 2, \dots, n$.

For proper operation, the DPP converter topology should be a bidirectional isolated topology. The advantage of this architecture is that each PV element's power can be exchanged directly with the independent bus that has a lower voltage than the bus voltage, which reduces component voltage ratings and cost. However, in order to maintain a stable voltage of the isolated bus, the power into and out of the bus must be equal, as in (6). This means that exact MPPT may not be achievable at any given string current, which is a trade-off of choosing this architecture.

Most of the research on the PV-IP architecture has focused on developing effective control algorithms for the DPP converters and mathematically proving stability. The first work was [32], which compared a non-isolated and isolated DPP topology, finding the isolated bidirectional flyback converter more effective. The proposed control was for each DPP converter to control the PV voltage based on the voltage of the isolated port, which achieves near-MPP tracking through voltage balancing. The implementation was for three sub-strings of a PV panel and three DPP converters connected to one isolated bus. Further studies in [11] investigated power-limited PV-IP converters and found that rating at 20–30% of the PV element power is effective. Similar work in [33] uses the same topology and setup, but proposes a voltage control strategy of each PV element based on the voltage difference between the PV element and the isolated bus. The control circuitry is simpler and lower-cost than the previous work and is aimed at IC implementation. Work in [34], also used the bidirectional flyback topology but implemented a fast control algorithm in the DPP converter to achieve exact MPP operation when specifically coordinated with a slower string-level inverter running MPPT. The implementation details for the PV-IP DPP systems are summarized in Table III.

D. Inverter Interaction

For DPP systems to be more easily adopted in grid-connected PV systems, their control system must properly interact with existing PV string inverters, as shown in Fig. 6. A string inverter would be used for a full-scale DPP system of many PV panels, but DPP can also be implemented for single panel where DPP converters compensate mismatch in the substrings and the inverter is a panel-level microinverter, typically used for residential applications. In both cases, commercial PV inverters typically run a standard extremum-seeking MPPT algorithm,

TABLE III
COMPARISON OF SERIES DPP PV-IP ARCHITECTURES

Flow	Topology	PV Control (MPPT accuracy)	Exp. Setup	Ref.
bidir.	flyback	V balance based on isolated port voltage (near)	3 PV, 3 DPP Conv.	[11], [32]
bidir.	flyback	V balance based on PV and isolated port voltage difference (near)	3 PV, 3 DPP Conv.	[33]
bidir.	flyback	distributed asynchronous MPPT (exact, with string MPPT)	3 PV, 3 DPP Conv.	[34]

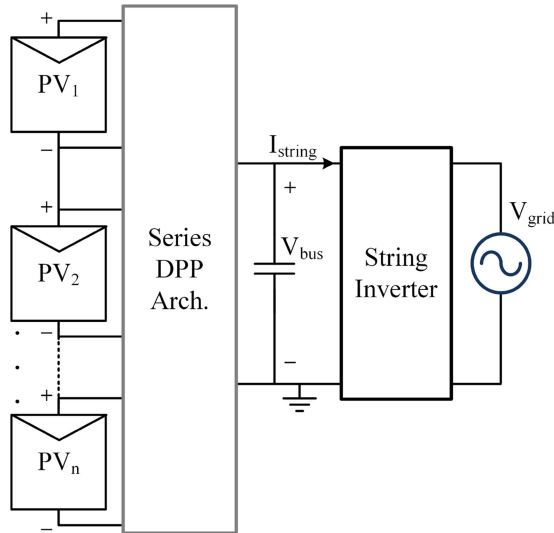


Fig. 6. Series DPP architecture with a grid-connect inverter.

such as P&O. These MPPT algorithms work most effectively with a smooth, convex power versus current (P-I) curve because it ensures that the PV string consistently operates at the system's true maximum. If there are multiple peaks in the P-I curve, which commonly occurs in partially-shaded series PV strings, the system may operate at a local maximum where PV power is not maximized.

The series DPP architectures are compared to investigate the shape of the power curve and the maximum output power. Simulation is used for direct comparison of the series string, conventional PV-bus with exact MPPT control, PV-PV with exact MPPT control, and PV-IP with voltage balance control. The simulation setup assumes four PV panels with the nominal MPP at 16 V and 9 A. The PV-bus and PV-IP has four isolated DPP converters and PV-PV has three nonisolated DPP converters. For the nonisolated PV-PV DPP converters, efficiency is assumed to be 92%. For the isolated PV-bus and PV-IP DPP converters, efficiency is assumed to be slightly lower at 85%. Each DPP converter is power limited such that it can process up to 3 A of current, which is 33% of the PV power rating. If the DPP converter reaches the current limit, the control target of exact MPPT control or voltage balancing cannot be achieved, but the system operates at the point closest to the target that meets the constraints of the DPP converter.

Two realistic irradiance data sets from an building-mounted PV application were used: one with relatively even light and the second with irradiance variation. The even irradiance set is 376, 406, 418, and 418 W/m² on each of the four PV elements, respectively. The uneven irradiance set is 733, 1236, 1240, and

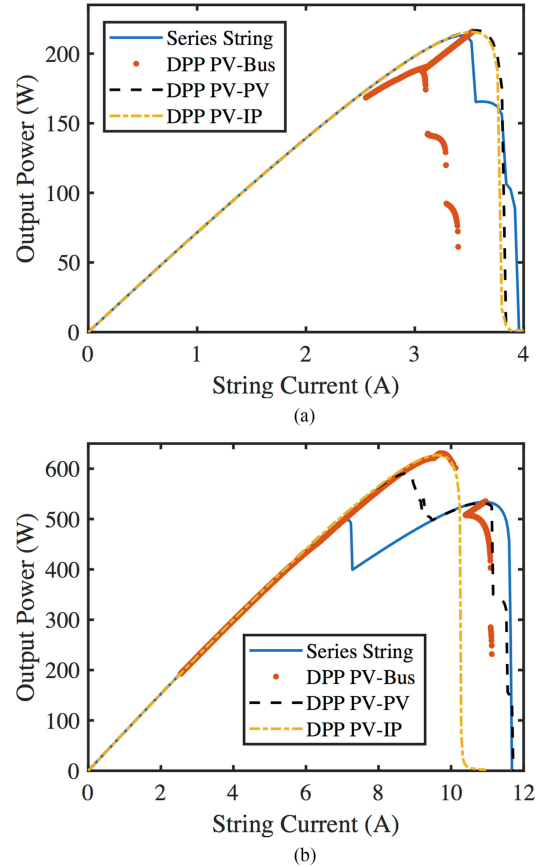


Fig. 7. P-I curve of series string and DPP architectures under (a) relatively even lighting and (b) partial shading.

TABLE IV
SERIES DPP ARCHITECTURE COMPARISON RESULTS

Light Setup	even 376 - 418 W/m ²		uneven 733 - 1240 W/m ²	
	power (W)	improvement (%)	power (W)	improvement (%)
S. Str.	213.1	0	534.0	0
PV-Bus	215.8	1.3	630.6	18.1
PV-PV	216.8	1.7	590.3	10.5
PV-IP	215.6	1.2	627.0	17.4

1240 W/m². This PV setup was simulated using Matlab to determine the steady-state operating point at a given inverter string current, and the string current was swept from 0 to the short-circuit current. The resulting P-I curves for series string and the three DPP architectures are shown in Fig. 7. Calculations of output power and improvement over the series string is shown in Table IV.

1) *Even Lighting Case*: Results for the even lighting case are shown in Fig. 7a, where irradiance is lower and only varies from 376 to 418 W/m². The curve for series string is not convex, but there this a global MPP around 3.5 A, where most extremum-seeking MPPT algorithms would successfully track. PV-PV and PV-IP exhibit smooth convex curves that allow for the inverter to consistently operate at the MPP.

For the PV-bus architecture under exact MPPT control, points shown are only for those where the value of current I_{ss} (shown in Fig. 2) is positive, as negative values of I_{ss} are not practical. As shown, PV-bus does not have a convex P-I curve and displays a linear region from 3.1 to 3.6 A. In this region, there are two solutions to the DPP system that achieve MPP operation and yield the same string current: one with a positive I_r (shown in Fig. 2) and the other with a negative I_r . Note that some string currents have two or even three potential solutions while other string currents have no solutions. Also, the 3.6-A global MPP has solutions at lower currents but no solutions at higher currents, meaning that exact MPPT cannot be achieved at currents higher than the MPP. With a extremely fast MPPT algorithm, the PV-bus architecture may not interact well with inverters due to the irregular shape of the P-I curve. The actual power curve of the PV-bus architecture depends on the specific implementation of the MPPT control. Thus, care must be taken in designing the PV-bus control algorithm to reach the global MPP, while ensuring a smooth power curve that interacts well with the inverter.

In terms of maximum output power in this case, the DPP architectures show a slight increase of 1.2–1.7% over series string. This relatively small increase is expected in even conditions, as series string is quite effective in even conditions. Still, the DPP architectures all show some improvement, with PV-PV exhibiting the highest improvement of 1.7%.

2) *Uneven Lighting Case*: Results for the uneven lighting case are shown in Fig. 7b, where one panel is shaded at 733 W/m² and the other three are in the range of 1236 to 1240 W/m². Due to the partial shading, the series string shows two distinct peaks where an extremum-seeking MPPT algorithm may operate at either the global maximum or the lower-power local maximum. The PV-IP with voltage balance control has a smooth convex shape such that the MPP will be effectively tracked. In this case, the PV-PV architecture does not have a convex shape and shows two distinct local maxima. This is due to the rating limitation of the DPP converter. Because the MPP of the four panels are significantly different, the PV-PV DPP converters are not able to fully compensate the difference, which results in reduced performance and multiple peaks in the power curve. Although the PV-PV architecture is able to reach 10.5% higher power than series string at the global maximum, the inverter MPPT algorithm may end up operating at the lower-power local maximum.

For the uneven light case, the PV-bus architecture with exact MPPT control again shows an irregular, nonconvex curve. However, the range of string currents with solutions (satisfying $I_{ss} > 0$) is wider than in the even lighting case. Because the difference in PV MPP currents is large, the 3-A current limit of the DPP converters is easily reached, which affects the P-I curve.

As a result, the curve is smoother below 10 A which includes the global MPP at 9.6 A, but the curve above 10 A is irregular and results in a lower-power local maximum point. Improved design of the PV-bus control algorithm is crucial for creating a smoother power curve without multiple peaks.

For maximum output power in the uneven lighting case, the DPP architectures show a more significant increase of 10.5–18.1% over series string. In this case, PV-PV exhibits the lowest improvement of 10.5%, while PV-bus exhibits the highest improvement of 18.1%. All DPP architectures exhibit a substantial power increase even with the DPP converter is rated at only 33% of the PV power.

3) *Summary*: Overall, all DPP architectures show higher output power performance than series string. There are narrower power gains in even irradiance conditions, but significant gains in uneven conditions. The PV-PI architecture with voltage balancing control consistently exhibits a convex power curve with good inverter interaction. Although it does not exhibit the highest output power compared to other DPP architectures, it shows consistent performance. The power curve of the PV-PV architecture with exact MPPT control is convex in even lighting conditions, but multiple peaks can form in uneven lighting conditions when the current limit of the DPP converters is reached. It is most effective for smaller numbers of panels [21] and in conditions where heavy partial shading is not expected. The PV-bus architecture with exact MPPT control has a nonconvex P-I curve, which is unfavorable for inverter interaction. For this reason, alternative control strategies are needed for the PV-bus architecture to create a convex P-I curve shape, while still reaching the global MPP. If this problem is overcome, the PV-bus architecture will be effective for larger numbers of panels [21] and in conditions with heavy partial shading.

E. Discussion

Although the concept of DPP for PV power has been around for a number of years and panel-level DPP has been shown to work with a commercial microinverter in [35], commercialization of DPP has not yet reached the market. In the PV market, up-front cost is a primary concern. For DPP systems to be competitive in the commercial market, they must have a system cost that is similar or lower than existing PV converter systems. As there are more components than series string and more complex control than FPP, this typically results in a higher up-front cost. Although DPP converters provide increased energy capturer over the lifetime compared to series string or FPP [21], many consumers still focus on initial investment cost rather than lifetime watts per dollar.

Another critical point for commercial adoption is long-term reliability. PV panels are rated for up to 20 years and maintenance labor costs are high, so reliability of PV converters is crucial. Because DPP is a relatively new technology, it has not yet endured long-term reliability testing. In general, PV converter companies do not readily adopt new technologies that are not fully mature. It is important to note that although DPP technologies have many components, their loading and resulting component wear is actually lower than FPP systems [12] such

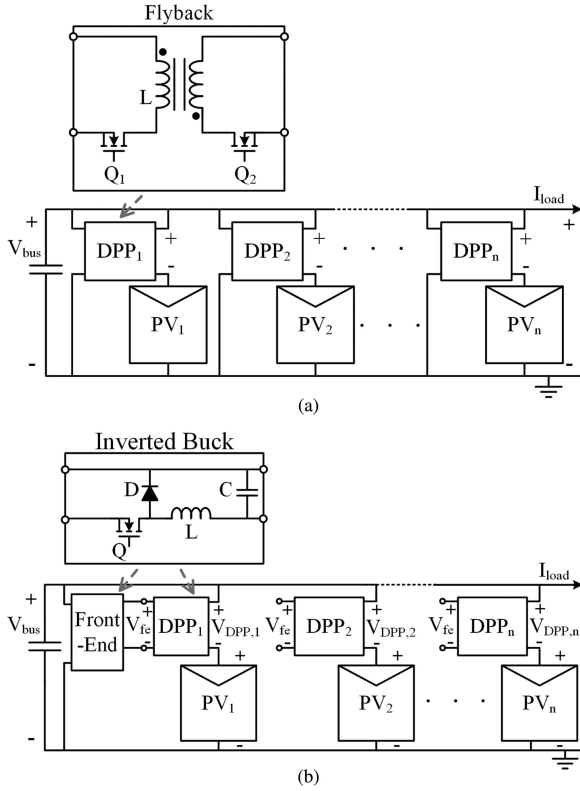


Fig. 8. Parallel DPP architectures (a) in direct connection with flyback DPP converters and (b) using a front-end converter with inverted buck converters.

that DPP systems have a lower expected failure rate. Further, if DPP systems fail they can be designed to have minimal negative impact on system operation such that the system still functions properly. For example, if a DPP converter fails and disconnects itself from the PV string, that PV segment operates as in series string and still provides its power to the load. Alternatively, various safety measures can be designed into DPP converters to adhere to changing safety standards, which is another critical driver in the PV market.

III. PARALLEL DPP

While series DPP converters are able to compensate for extreme light differences, in some unfavorable cases, they must process a significant amount of power to achieve individual MPPT [21], which takes away from the fundamental advantage of the DPP approach. An alternative DPP architecture is to use parallel DPP converters, as shown in Fig. 8. In a parallel DPP system, the PV voltage and bus voltage V_{bus} are related according to

$$V_{bus} = V_{PV,k} + V_{DPP,k} \quad (8)$$

for $k = 1, 2, \dots, n$, where $V_{DPP,k}$ is the output voltage of the k th DPP converter. Then, load current of an ideal system is

$$I_{load} = \sum_{k=1}^n I_{PV,k} \frac{V_{PV,k}}{V_{bus}} \quad (9)$$

Instead of the DPP converters offsetting current from a common current as in series DPP, parallel DPP converters offset

voltage from a common voltage bus. Based on the operating characteristics of PV cells, the voltage characteristics are less sensitive to extreme light differences than the current characteristics [38]–[40]. This indicates that when extreme light differences are expected, parallel connection is more advantageous for maximizing PV power.

The main advantage of parallel DPP systems is its high system efficiency, when properly designed with the PV element voltage close to the dc bus voltage. Each PV cell is able to operate at its MPP under any lighting condition, while the processed power and resulting power loss in the converters is proportional to the voltage difference between the PV element and the dc bus. Thus far, only a few approaches to implementing parallel DPP converters have been reported in the literature. There are two main parallel DPP architectures: direct connection and with a front-end converter.

A. Direct Connection

The direct parallel DPP architecture is shown in Fig. 8a. Authors in [36], referring to parallel DPP converters as PV balancers, used a flyback converter for the direct parallel DPP converter. The flyback converter is not used to provide input-output isolation, as the positive side of the input and output are directly connected; it is used because it is one of the few topologies that achieves DPP in this architecture. Note that a topology such as the inverted (low-side) buck converter may seem appropriate at first glance, but it is actually equivalent to a FPP boost converter and is not an appropriate DPP topology. For the direct parallel DPP converter, a large voltage step-down ratio is required. Thus, the coupled inductor turns ratio in the flyback can be utilized for this goal, but achieving high efficiency is difficult.

B. With a Front-End Converter

The other parallel DPP architecture with a front-end converter is shown in Fig. 8b. The front-end converter steps down the bus voltage to an intermediate voltage level, which becomes the input of the DPP converters. Although isolated topologies could be used for this architecture, non-isolated converters with higher efficiency are more appropriate. Work in [36] used inverted buck converters for both the front-end and parallel DPP converters. For a residential PV application, cost analysis showed that this architecture with the inverted buck topology was more cost effective and showed similar performance to that of the direct parallel DPP architecture. Work in [37] also implemented the architecture with a front-end converter but for a lower-power energy harvesting PV application with extreme uneven lighting expected over four PV cells. The inverted buck converter was used for both the front-end and DPP converters and P&O MPPT was implemented to achieve individual MPP operation.

C. Discussion

The implementation details for the parallel DPP systems are summarized in Table V. For these parallel DPP architectures, converters are unidirectional which makes their design simpler

TABLE V
COMPARISON OF PARALLEL DPP ARCHITECTURES

Architecture	Topology	PV Control (MPPT accuracy)	Exp. Setup	Ref.
direct	flyback	unspecified MPPT (exact)	3 PV, 3 DPP Conv.	[36]
with front-end	inverted buck	unspecified MPPT (exact)	3 PV, 3 DPP Conv.	[36]
with front-end	inverted buck	P&O MPPT (exact)	4 PV, 4 DPP Conv.	[37]

than bidirectional converters used in series DPP architectures. Parallel DPP architectures are highly effective at maximizing power even under extreme light differences [41], but are most appropriate when the PV element voltage is similar to the load voltage. At present, only a few topologies for parallel DPP converters have been implemented, but it is an area open for further research.

IV. CONCLUSION

Since the DPP concept for PV systems was introduced in recent years, various work has been developed and published in the literature. The advantages of higher output power, lower converter cost, and better system reliability in DPP PV systems compared to series string and FPP converters have been outlined. Most existing research has focused on series DPP architectures, which includes PV-bus, PV-PV, PV-IP, and a number of variations.

For the conventional PV-bus architecture with MPPT control, there are inverter interaction challenges, but variations of the PV-bus architecture have been successfully implemented. A number of unidirectional bus-to-PV converter topologies have been used to achieve voltage balancing of the PV elements, and the PV-bus-direct architecture uses an additional string converter to achieve MPPT of the PV elements but also processes more power through the string converter. The PV-PV architecture is the most widely implemented with either the switch inductor or resonant switched capacitor topology. Various control schemes have been developed for both voltage balancing and exact MPPT of the PV elements, with effective inverter MPPT algorithm interaction when the rating limit of the PV-PV converter is not reached. The PV-IP architecture has been implemented using flyback converters and both voltage balance and MPPT algorithms have been developed. PV-IP DPP systems have been shown to work most consistently with standard inverter MPPT algorithms.

Through the literature and comparative simulation, series DPP architectures have shown better performance than series string and FPP converters, and various control strategies have been proposed that are well-suited for grid-connected PV inverter applications. Parallel DPP is less studied in the literature, but shows promise for lower-voltage and emerging PV applications. For parallel DPP architectures, the direct DPP converter connection and approach with a front-end converter have been shown to effectively achieve MPPT of each PV element. The PV DPP system architectures, topologies, and control approaches currently available in the literature have been overviewed and their advantages and trade-offs have been discussed. Continued research on PV DPP is still needed for scalable systems,

development for commercialization, long-term reliability, and emerging PV applications.

REFERENCES

- [1] F. Blaabjerg, Y. Yang, D. Yang, and X. Wang, "Distributed power-generation systems and protection," *Proc. IEEE*, vol. 105, no. 7, pp. 1311–1331, Jul. 2017.
- [2] T. V. Tran and W. Y. Chung, "High-efficient energy harvester with flexible solar panel for a wearable sensor device," *IEEE Sens. J.*, vol. 16, no. 24, pp. 9021–9028, Dec. 2016.
- [3] H. Patel and V. Agarwal, "MATLAB-based modeling to study the effects of partial shading on PV array characteristics," *IEEE Trans. Energy Convers.*, vol. 23, no. 1, pp. 302–310, Mar. 2008.
- [4] P. Manganiello, M. Balato, and M. Vitelli, "A survey on mismatching and aging of PV modules: The closed loop," *IEEE Trans. Ind. Electron.*, vol. 62, no. 11, pp. 7276–7286, Nov. 2015.
- [5] K. A. Kim and P. T. Krein, "Reexamination of photovoltaic hot spotting to show inadequacy of the bypass diode," *IEEE J. Photovolt.*, vol. 5, no. 5, pp. 1435–1441, Sep. 2015.
- [6] G. R. Walker and P. C. Sernia, "Cascaded DC-DC converter connection of photovoltaic modules," *IEEE Trans. Power Electron.*, vol. 19, no. 4, pp. 1130–1139, Jul. 2004.
- [7] S. M. Chen, T. J. Liang, and K. R. Hu, "Design, analysis, and implementation of solar power optimizer for DC distribution system," *IEEE Trans. Power Electron.*, vol. 28, no. 4, pp. 1764–1772, Apr. 2013.
- [8] Y. Fang and X. Ma, "A novel PV microinverter with coupled inductors and double-boost topology," *IEEE Trans. Power Electron.*, vol. 25, no. 12, pp. 3139–3147, Dec. 2010.
- [9] M. Balato and M. Vitelli, "A new control strategy for the optimization of distributed MPPT in PV applications," *Int. J. Elect. Power Energy Syst.*, vol. 62, pp. 763–773, 2014.
- [10] M. Vitelli, "On the necessity of joint adoption of both distributed maximum power point tracking and central maximum power point tracking in PV systems," *Prog. Photovolt., Res. Appl.*, vol. 22, no. 3, pp. 283–299, 2012.
- [11] C. Olalla, C. Deline, D. Clement, Y. Levron, M. Rodriguez, and D. Maksimovic, "Performance of power-limited differential power processing architectures in mismatched PV systems," *IEEE Trans. Power Electron.*, vol. 30, no. 2, pp. 618–631, Feb. 2015.
- [12] P. S. Shenoy, K. A. Kim, B. B. Johnson, and P. T. Krein, "Differential power processing for increased energy production and reliability of photovoltaic systems," *IEEE Trans. Power Electron.*, vol. 28, no. 6, pp. 2968–2979, Jun. 2013.
- [13] P. S. Shenoy and P. T. Krein, "System and method for optimizing solar power conversion," U.S. Patent 8 508 074 B2, Aug. 13, 2013.
- [14] T. Shimizu, M. Hirakata, T. Kamezawa, and H. Watanabe, "Generation control circuit for photovoltaic modules," *IEEE Trans. Power Electron.*, vol. 16, no. 3, pp. 293–300, May 2001.
- [15] C. Olalla, M. N. Hasan, C. Deline, and D. Maksimovic, "Mitigation of hot-spots in photovoltaic systems using distributed power electronics," *Energies*, vol. 11, no. 4, pp. 1–16, Mar. 2018, Art. no. 726.
- [16] J. Biswas, A. K. M, A. K. G., and M. Barai, "Design, architecture and real time distributed coordination DMPPT algorithm for PV systems," *IEEE J. Emerg. Sel. Topic Power Electron.*, vol. 6, no. 3, pp. 1418–1433, Sep. 2018.
- [17] M. Uno and A. Kukita, "Two-switch voltage equalizer using an LLC resonant inverter and voltage multiplier for partially shaded series-connected photovoltaic modules," *IEEE Trans. Ind. Appl.*, vol. 51, no. 2, pp. 1587–1601, Mar. 2015.
- [18] M. Uno and A. Kukita, "Current sensorless equalization strategy for a single-switch voltage equalizer using multistacked buck-boost converters for photovoltaic modules under partial shading," *IEEE Trans. Ind. Appl.*, vol. 53, no. 1, pp. 420–429, Jan. 2017.

- [19] Y. T. Jeon, H. Lee, K. A. Kim, and J. H. Park, "Least power point tracking method for photovoltaic differential power processing systems," *IEEE Trans. Power Electron.*, vol. 32, no. 3, pp. 1941–1951, Mar. 2017.
- [20] Y. T. Jeon and J. h. Park, "Unit-minimum least power point tracking for the optimization of photovoltaic differential power processing systems," *IEEE Trans. Power Electron.*, to be published, doi: [10.1109/TPEL.2018.2822289](https://doi.org/10.1109/TPEL.2018.2822289).
- [21] K. A. Kim, P. S. Shenoy, and P. T. Krein, "Converter rating analysis for photovoltaic differential power processing systems," *IEEE Trans. Power Electron.*, vol. 30, no. 4, pp. 1987–1997, Apr. 2015.
- [22] M. Badawy and Y. Sozer, "Differential power processing of photovoltaic systems for high energy capture and reduced cost," in *Proc. IEEE Energy Convers. Congr. Expo.*, Oct. 2017, pp. 475–481.
- [23] L. F. L. Villa, T. P. Ho, J. C. Crebier, and B. Raison, "A power electronics equalizer application for partially shaded photovoltaic modules," *IEEE Trans. Ind. Electron.*, vol. 60, no. 3, pp. 1179–1190, Mar. 2013.
- [24] H. J. Bergveld *et al.*, "Module-level DC/DC conversion for photovoltaic systems: The delta-conversion concept," *IEEE Trans. Power Electron.*, vol. 28, no. 4, pp. 2005–2013, Apr. 2013.
- [25] M. S. Zaman *et al.*, "A cell-level differential power processing IC for concentrating-PV systems with bidirectional hysteretic current-mode control and closed-loop frequency regulation," *IEEE Trans. Power Electron.*, vol. 30, no. 12, pp. 7230–7244, Dec. 2015.
- [26] S. Qin, S. T. Cady, A. D. Dominguez-Garcia, and R. C. N. Pilawa-Podgurski, "A distributed approach to maximum power point tracking for photovoltaic submodule differential power processing," *IEEE Trans. Power Electron.*, vol. 30, no. 4, pp. 2024–2040, Apr. 2015.
- [27] F. Wang, T. Zhu, F. Zhuo, and H. Yi, "An improved submodule differential power processing-based PV system with flexible multi-MPPT control," *IEEE J. Emerg. Sel. Topic Power Electron.*, vol. 6, no. 1, pp. 94–102, Mar. 2018.
- [28] J. T. Stauth, M. Seeman, and K. Kesarwani, "Resonant switched-capacitor converters for sub-module distributed photovoltaic power management," *IEEE Trans. Power Electron.*, vol. 28, no. 3, pp. 1189–1198, Mar. 2013.
- [29] A. Blumenfeld, A. Cervera, and M. M. Peretz, "Enhanced differential power processor for PV systems: Resonant switched-capacitor gyrator converter with local MPPT," *IEEE J. Emerg. Sel. Topic Power Electron.*, vol. 2, no. 4, pp. 883–892, Dec. 2014.
- [30] Z. Qiu and K. Sun, "A photovoltaic generation system based on wide voltage-gain DC-DC converter and differential power processors for DC microgrids," *Chin. J. Elect. Eng.*, vol. 3, no. 1, pp. 84–95, Jun. 2017.
- [31] T. Eram and P. L. Chapman, "Comparison of photovoltaic array maximum power point tracking techniques," *IEEE Trans. Energy Convers.*, vol. 22, no. 2, pp. 439–449, Jun. 2007.
- [32] C. Olalla, D. Clement, M. Rodriguez, and D. Maksimovic, "Architectures and control of submodule integrated DC-DC converters for photovoltaic applications," *IEEE Trans. Power Electron.*, vol. 28, no. 6, pp. 2980–2997, Jun. 2013.
- [33] Y. Levron, D. Clement, B. Choi, C. Olalla, and D. Maksimovic, "Control of submodule integrated converters in the isolated-port differential power-processing photovoltaic architecture," *IEEE J. Emerg. Sel. Topic Power Electron.*, vol. 2, no. 4, pp. 821–832, Dec. 2014.
- [34] R. Bell and R. C. N. Pilawa-Podgurski, "Decoupled and distributed maximum power point tracking of series-connected photovoltaic submodules using differential power processing," *IEEE J. Emerg. Sel. Topic Power Electron.*, vol. 3, no. 4, pp. 881–891, Dec. 2015.
- [35] S. Qin, C. B. Barth, and R. C. N. Pilawa-Podgurski, "Enhancing microinverter energy capture with submodule differential power processing," *IEEE Trans. Power Electron.*, vol. 31, no. 5, pp. 3575–3585, May 2016.
- [36] H. Zhou, J. Zhao, and Y. Han, "PV balancers: Concept, architectures, and realization," *IEEE Trans. Power Electron.*, vol. 30, no. 7, pp. 3479–3487, Jul. 2015.
- [37] H. Lee and K. A. Kim, "Differential power processing converter design for photovoltaic wearable applications," in *Proc. Int. Power Electron. Motion Control Conf.*, May 2016, pp. 463–468.
- [38] M. G. Villalva, J. R. Gazoli, and E. Filho, "Comprehensive approach to modeling and simulation of photovoltaic arrays," *IEEE Trans. Power Electron.*, vol. 24, no. 5, pp. 1198–1208, May 2009.
- [39] K. A. Kim, C. Xu, J. Lei, and P. T. Krein, "Dynamic photovoltaic model incorporating capacitive and reverse-bias characteristics," *IEEE J. Photovolt.*, vol. 3, no. 14, pp. 1334–1341, Oct. 2013.
- [40] D. Jena and V. V. Ramana, "Modeling of photovoltaic system for uniform and non-uniform irradiance: A critical review," *Renewable Sustain. Energy Rev.*, vol. 52, pp. 400–417, 2015.
- [41] H. Lee and K. A. Kim, "Comparison of photovoltaic converter configurations for wearable applications," in *Proc. Workshop Control Model. Power Electron.*, Jul. 2015, pp. 1–6.



Hoejeong Jeong (S'17) received the B.S. degree in electrical engineering from the Ulsan National Institute of Science and Technology (UNIST), Ulsan, South Korea, in 2017. She is currently working toward the M.S. degree in electrical engineering with UNIST. Her research interests include dc-dc converter design and optimization for photovoltaic applications. She was the recipient of the Outstanding Undergraduate Student Award from the Korean Institute of Electrical Engineers in 2017.



Hyunji Lee (S'14) received the B.S. and M.S. degrees in electrical engineering from the Ulsan National Institute of Science and Technology, Ulsan, South Korea, in 2015 and 2017, respectively. She is working as an Assistant Engineer with Fine Inc., Seoul, South Korea. Her research interests include design and analysis of differential power processing systems for photovoltaic applications.



Yu-Chen Liu (S'12–M'16–SM'18) received the B.S. and Ph.D. degrees in electrical engineering from the National Taiwan University of Science and Technology (NTUST), Taipei, Taiwan, in 2009 and 2015, respectively. He was a Visiting Researcher with the Future Energy Electronics Center, Virginia Tech., Blacksburg, VA, USA, in 2014. From 2015 to 2016, he was a Research Assistant Professor with the Department of Electronic Engineering, NTUST, for the Power Electronics Laboratory. He is currently an Assistant Professor with the Department of Electrical Engineering, National Ilan University, Yilan, Taiwan. His research interests include analysis and design of zero-voltage-switching dc-dc converters, power factor correction techniques, redundant server power supplies, and high-frequency converter designs.

Dr. Liu was the recipient of the Young Researcher Award in 2018 from the National Science Council of Taiwan. He was a Faculty Advisor for student teams of the IEEE International Future Energy Challenge, receiving Awards in 2015, 2016, and 2017. He serves as the Chair of the IEEE Industrial Applications Society Taipei Chapter for 2017–2018.



Katherine A. Kim (S'06–M'14–SM'18) received the B.S. degree in electrical and computer engineering from the Franklin W. Olin College of Engineering, Needham, MA, USA, in 2007. She received the M.S. and Ph.D. degree in electrical and computer engineering from the University of Illinois, Urbana-Champaign, IL, USA, in 2011 and 2014, respectively. Since 2014, she has been a Faculty Member with the School of Electrical and Computer Engineering, Ulsan National Institute of Science and Technology (UNIST), Ulsan, South Korea, and is currently an Associate Professor. Her research interests are power electronics, modeling, and control for photovoltaic and energy harvesting applications.

Dr. Kim received the National Science Foundation's East Asia and Pacific Summer Institutes Fellowship in 2010 and Graduate Research Fellowship in 2011. She was the Chair of the IEEE Power and Energy Society (PES)/Power Electronics Society (PELS) Joint Student Chapter at the University of Illinois, in 2010–2011, and the Co-Director of the IEEE Power and Energy Conference at Illinois, in 2012. Since 2017, she has been an Associate Editor for the IEEE TRANSACTIONS ON POWER ELECTRONICS, since 2017. She was the IEEE PELS Student Membership Chair, in 2013–2014, the IEEE PELS Women In Engineering Chair in 2018, and an IEEE PELS Member-at-Large for 2016–2018.